[CrFCl(en)(tn)]Cl it is necessary to heat the complex a very long time (24 h at 130 °C). Following the Tsuchiya theory,[14,15] this isomerization undoubtedly takes place with the Cr–N(amine) bond rupture to give a pentacoordinate species, because there is no water in the coordination of Cr(III). Taking into account the absence of the chx ligand, this rupture is very difficult and it needs either high temperature or a long time (as is the experimental fact).

On the other hand, in the chx–tn series, the variation of the E_a values is not linear with the size of the entering anion (as occurs in the other series) (Figure 2). The possible explanation is to suppose, specifically, that the Cr–N(chx) bond rupture has a different extent depending on the entering anion.

The other kinetic parameters follow the same variation as E_a (Table IV). ΔS^* is a measurement of the distortion in the lattice in forming the activated complex.[3] If we suppose the Cr–N(chx) bond rupture, the monodentate chx amine creates more distortion by free rotation and increases the ΔS^*. The frequency factor, k_0, indicates, according to the literature,[16,17] the rigidity of the activated complex. Greater k_0 indicates greater mobility in the activated complex. The *trans*-[CrF(en)(tn)(H_2O)]Cl_2, which does not show isomerization, has a very small value of k_0. The activated complex is, consequently, very rigid, and the anion entrance in the same position from which the water molecule is lost would be very easy.

From all the results obtained with the TG and DSC measurements we can deduce that the activation parameters (over all the low values of E_a) (Table IV) are in agreement with a dissociative mechanism for all these reactions,[1,2] with the formation of a pentacoordinate intermediate. In the en–tn series, this pentacoordinate intermediate is due to the loss of the water molecule. The external anion can enter in the cis or trans position depending on the mobility of this activated complex. In the chx–tn series, instead, the mechanism (although dissociative) is somewhat different. There are two possible pentacoordinate intermediates: one created by the loss of the water molecule and the other created by the Cr–N(chx) bond rupture.

Conclusion

The results reported here confirm, once more, the importance of the ratio of anion/cation volume and the importance of the compacity in the packing, which is the so-called "free-space theory". On the other hand, the low values of E_a in all the complexes support the dissociative mechanism in this kind of solid-state reactions, as was previously predicted by House and LeMay.[3,20]

Acknowledgment. The computational part of this work was supported by the CAICYT through Grant 0657/81.

Registry No. *trans*-[CrFCl(en)(tn)]Cl, 96482-47-2; [CrFCl(en)(tn)]Cl, 96554-58-4; [CrFBr(en)(tn)]Br, 96554-55-1; [CrFI(en)(tn)]I, 109864-08-6; [CrF(S_2O_6)(en)(tn)], 109889-32-9; [CrFCl(tn)(chx)]Cl, 109864-09-7; [CrFBr(tn)(chx)]Br, 109864-10-0; [CrFI(tn)(chx)]I, 109864-11-1; [CrF(S_2O_6)(tn)(chx)], 109864-12-2; *trans*-[CrF(en)(tn)(H_2O)]Cl_2, 96482-40-5; *trans*-[CrF(en)(tn)(H_2O)]Br_2, 96482-41-6; *trans*-[CrF(en)(tn)(H_2O)]I_2, 96482-39-2; *trans*-[CrF(en)(tn)(H_2O)]S_2O_6, 109864-13-3; *trans*-[CrF(tn)(chx)(H_2O)]Cl_2, 109864-14-4; *trans*-[CrF(tn)(chx)(H_2O)]Br_2, 109864-15-5; *trans*-[CrF(tn)(chx)(H_2O)]I_2, 109864-16-6; *trans*-[CrF(tn)(chx)(H_2O)]S_2O_6, 109864-17-7; *trans*-[CrF_2(en)(tn)]Br, 97107-81-8; *trans*-[CrF_2(tn)(chx)]Br, 109864-18-8; *trans*-[CrF(en)(tn)(H_2O)](ClO_4)$_2$, 96482-38-1; *trans*-[CrF(chx)(tn)(H_2O)](ClO_4)$_2$, 106676-16-8.

---

(16) Cordes, H. I. *J. Phys. Chem.* **1968**, *72*, 2187.
(17) Shannon, R. P. *Trans. Faraday Soc.* **1964**, *60*, 1902.
(18) Bamford, D. H., Ed. *Comprehensive Chemical Kinetics*; Elsevier: Amsterdam, 1980; Vol. 22, Chapter 3.
(19) Basolo, F. Pearson, R. G. *Mechanism of Inorganic Reactions*, 2nd ed.; Wiley: New York, 1962; Chapter 3.
(20) LeMay, H. E.; Babich, M. W. *Thermochim. Acta* **1981**, *48*, 147.

Contribution from the Department of Chemistry,
Faculty of Science, University of Kuwait, Kuwait, Kuwait

Electronic Structure and Ligand Field States of $NpO_2Cl_4^{2-}$ and $NpO_2(NO_3)_3^-$: A Relativistic MS-Xα Study

M. A. Makhyoun*

Received December 23, 1986

Relativistic MS-Xα calculations are reported for two neptunyl complexes: $NpO_2Cl_4^{2-}$ and $NpO_2(NO_3)_3^-$. From the MS-Xα results a perturbation method is used to set up simultaneous ligand field + spin–orbit coupling matrices for the f^1 system. The predicted symmetries and energies of the f–f transitions are in good agreement with experiment. The ligand field parameters obtained in this work for $NpO_2Cl_4^{2-}$ are compared with those of UCl_6^- and $PaCl_6^{2-}$ derived from other Xα calculations.

Introduction

The quasi-relativistic MS-Xα method (RXα) has been applied successfully to many molecules,[1-5] since the work of Boring et al. on the uranyl ion,[6] UO_2^{2+}. The development of the method to include the mass-velocity and Darwin terms necessary for treating molecules containing heavy atoms is due to Wood and Boring.[7] Their approach is based on the scheme described by Cowan and Griffin[8] for the solution of the Dirac–Hartree–Fock equation.

In this work the relativistic Xα spin–orbit coupling free Hamiltonian was used to obtain the SCF ground-state electronic structures of $NpO_2Cl_4^{2-}$ and $NpO_2(NO_3)_3^-$ ions.

Many attempts[9-11] have been elaborated in order to combine the Xα method with ligand field theory to obtain a proper description of the electronic d–d transitions of metal complexes. Good results have been obtained recently[12] for $CrCl_6^{3-}$ and CrF_6^{3-} ions from a direct evaluation of the Griffith electron repulsion parameters necessary for describing the energies of the ligand field

---

* To whom correspondence should be addressed at the Department of Chemistry, Faculty of Science, University of Alexandria, Alexandria, Egypt.

(1) Koelling, D. D.; Ellis, D. E.; Bartlett, R. J. *J. Chem. Phys.* **1976**, *6*, 3331.
(2) Boring, M.; Wood, J. H. *J. Chem. Phys.* **1979**, *71*, 32.
(3) Thornton, G.; Rösch, N.; Edelstein, N. M. *Inorg. Chem.* **1980**, *19*, 1304.
(4) Hohl, D.; Rösch, N. *Inorg. Chem.* **1986**, *25*, 2711.
(5) El-Issa, B. D.; Makhyoun, M. A.; Salsâ, B. A. *Int. J. Quantum Chem.* **1987**, *31*, 295.
(6) Boring, M.; Wood, J. H.; Moskowitz, J. W. *J. Chem. Phys.* **1975**, *63*, 638.
(7) Wood, J. H.; Boring, A. M. *Phys. Rev. B: Condens. Matter* **1978**, *18*, 2701.
(8) Cowan, R. D.; Griffin, D. C. *J. Opt. Soc. Am.* **1976**, *66*, 1010.
(9) Sambe, H.; Felton, R. H. *Int. J. Quantum Chem.* **1976**, *10*, 155.
(10) Weber, J.; Daul, C. *Mol. Phys.* **1980**, *39*, 1001.
(11) Makhyoun, M. A.; Le Beuze, A.; Lissillour, R.; Chermete, H. *Theor. Chim. Acta* **1983**, *63*, 383.
(12) Goursot, A.; Daul, C. *NATO ASI Ser., Ser. C* **1986**, *No. 176*, 199.

0020-1669/87/1326-3592$01.50/0 © 1987 American Chemical Society

Table I. Geometry, Sphere Radii, and Exchange Parameters

$NpO_2(NO_3)_3^-$ (D_{3h})

Bond Distances (Å)

Np–O_2	2.469	N–O_2	1.283
Np–O_1[a]	1.732	N–O_3	1.199

Bond Angles (deg)

∠O_1–Np–O_1	180	∠O_2–N–O_2	115
∠O_2–Np–O_2	52	∠O_2–N–O_3	122.5

	sphere radius, Å	α		sphere radius, Å	α
Np	1.3333	0.69160	O_3	0.8586	0.74447
O_1	0.9139	0.74447	N	0.7697	0.75197
O_2	0.8806	0.74447	OUT	4.9653	0.73738

Watson sphere radius 4.9653; Watson sphere charge 1+

$NpO_2Cl_4^{2-}$ (D_{4h})

Bond Distances (Å)

Np–O	1.75	Np–Cl	2.61

Bond Angles (deg)

∠O–Np–O	180	∠Cl–Np–Cl	90

	sphere radius, Å	α
Np	1.3400	0.69160
O	0.9208	0.74447
Cl	1.4316	0.72325
OUT 4.0416	4.0416	0.72009

Watson sphere radius 4.0416; Watson sphere charge 2+

[a] O_1 refers to the oxygen in the NpO_2^{2+} ion while O_2 and O_3 are the oxygen atoms of the nitrate group. O_2 is the one that is directly bonded to Np.

multiplet states. The f–f transitions of the actinide complexes of O_h symmetry were also calculated properly within the RXα transition-state method.[1-3]

The spin–orbit coupling parameter of the 5f orbitals in the actinide series is comparatively large (ζ = 1600–2700 cm^{-1})[13] and should be included in any treatment regarding the electronic transitions within the f-orbital manifold.[14]

A detailed study of the single-crystal absorption and MCD spectra of $Cs_2U(Np)O_2Cl_4$ and $CsU(Np)O_2(NO_3)_3$[15] provides good information to test the ability of the RXα method for evaluating the possible f–f transitions in these systems.

In this study we attempt to apply the relativistic Xα method in combination with ligand field theory to systems of symmetry lower than cubic.

Method of Calculations

The geometry of $NpO_2(NO_3)_3^-$ was taken from the X-ray data[16] of $RbNpO_2(NO_3)_3$ idealized to D_{3h} symmetry. The bond lengths and angles of $NpO_2Cl_4^{2-}$ (D_{4h}) are estimated on the basis of the structures of $NpO_2(NO_3)_3^-$, $UO_2(NO_3)_3^-$, and $UO_2Cl_4^{2-}$ ions.[16-18] A summary of the structures of both ions is given in Table I.

The updated version of the SCF MS-Xα program[19] was used to calculate the electronic structures of $NpO_2Cl_4^{2-}$ and $NpO_2(NO_3)_3^-$ complexes. The computational details concerning the relativistic version used in this study can be found in other works.[5,7]

The atomic exchange factor α for Np was taken from ref 3; the other α values were taken from the compilation of Schwarz.[20] A weighted average of these atomic values was used for the interatomic and extramolecular regions. The Norman criteria[21] were used in choosing the atomic radii scaled by a factor of 0.88. An external tangent outer sphere was used, which also served as a Watson sphere on which a positive charge is distributed counter to the charge of the ion. Partial waves up to l = 4 were included in the outer sphere, l = 3 in the Np sphere, l = 2 in the chlorine sphere, and l = 1 for oxygen and nitrogen. The valence shells in this calculation include the following: for Np, 6s, 6p, and 5f; for O, 2s and 2p; for Cl, 3s and 3p; for N, 2s and 2p. A summary of these parameters is given in Table I.

Table II. Xα Eigenvalues and Major Atomic Populations of $NpO_2Cl_4^{2-}$[a]

sym D_{4h}	E, Ry		axial sym $D_{\infty h}$
$5a_{2u}$	−0.0604	0.577 Np(f) + 0.355 O(s)	$4\sigma_u^+$
$7e_u$	−0.2734	0.738 Np(f) + 0.212 O(p)	$3\pi_u + 1\phi_u$
$6e_u$	−0.3829	0.843 Np(f) + 0.120 Cl(p)	
$2b_{2u}$	−0.4001	0.943 Np(f) + 0.045 Cl(p)	$1\delta_u$
$1b_{1u}$	−0.4083	0.998 Np(f)	
Cl 3p-like MOs			
$3e_u$	−0.7482	0.289 Np(f) + 0.676 O(p)	$2\pi_u$
$1e_g$	−0.7506	0.156 Np(d) + 0.770 O(p)	$1\pi_g$
$3a_{2u}$	−0.7545	0.521 Np(f) + 0.326 O(p)	$3\sigma_u^+$
$4a_{1g}$	−0.9361	0.209 Np(d) + 0.709 O(p)	$3\sigma_g^+$
$2a_{2u}$	−1.4217	0.258 Np(p) + 0.514 O(p) +0.21 O(p)	$2\sigma_u^+$
Cl 3s-like MOs			
$1e_u$	−1.8452	0.891 Np(p) + 0.050 Cl(s)	$1\pi_u$
$2a_{1g}$	−1.9035	0.162 Np(d) + 0.755 O(s)	$2\sigma_g^+$
$1a_{2u}$	−2.4858	0.463 Np(p) + 0.339 O(s) + 0.140 O(p)	$1\sigma_u^+$
$1a_{1g}$	−3.6487	0.925 Np(s) + 0.031 O(s)	$1\sigma_g^+$

[a] Only MOs localized on the NpO_2^{2+} moiety are shown.

Table III. Xα Eigenvalues and Major Atomic Populations of $NpO_2(NO_3)_3^-$[a]

sym D_{3h}	E, Ry		axial sym $D_{\infty h}$
$7a_2''$	−0.2450	0.340 Np(p) + 0.470 Np(f) + 0.100 O_1(p)	$4\sigma_u^+$
$12e'$	−0.5703	0.693 Np(f) + 0.282 O_1(p)	$3\pi_u$
$5a_2'$	−0.6732	0.725 Np(f) + 0.243 O_2(p) + 0.285 O_3(p)	$1\phi_u$(a)
$5e''$	−0.7261	0.965 Np(f) + 0.030 O_3(p)	$1\delta_u$
$9a_1'$	−0.7283	0.993 Np(f)	$1\phi_u$(b)
$2e''$	−1.0179	0.170 Np(d) + 0.978 O_1(p)	$1\pi_g$
$8e'$	−1.0468	0.344 Np(f) + 0.619 O_1(p)	$2\pi_u$
$4a_2''$	−1.0877	0.118 Np(p) + 0.525 Np(f) + 0.328 O_1(p)	$3\sigma_u^+$
$7a_1'$	−1.2708	0.196 Np(d) + 0.788 O_1(s) + 0.695 O_1(p)	$3\sigma_g^+$
$2a_2''$	−1.7049	0.243 Np(p) + 0.541 O_1(s) + 0.189 O_1(p)	$2\sigma_u^+$
$4e'$	−2.1467	0.872 Np(p) + 0.036 O_2(p)	$1\pi_u$
$4a_1'$	−2.2569	0.062 Np(s) + 0.194 Np(d) + 0.677 O_1(s)	$2\sigma_g^+$
$1a_2''$	−2.9494	0.447 Np(p) + 0.310 O_1(s) + 0.170 O_1(p)	$1\sigma_u^+$
$1a_1'$	−4.0138	0.906 Np(s) + 0.040 O_1(s) + 0.043 O_1(p)	$1\sigma_g^+$

[a] Only MOs localized on the NpO_2^{2+} moiety are shown.

Results and Discussion

The relativistic SCF–Xα ground-state valence levels of $NpO_2Cl_4^{2-}$ and $NpO_2(NO_3)_3^-$ and the corresponding charge distribution are reported in Tables II and III, respectively. To correlate the electronic structure of these complexes with NpO_2^{2+}-like ions, the axial symmetry labels ($D_{\infty h}$) for the MOs localized on the NpO_2^{2+} moiety are also shown in Tables II and III. Note that the numbering of levels starts at the Np 6s-like MO. The calculations indicate the following ground-state orbital populations in the Np sphere:

$$NpO_2Cl_4^{2-}\text{:}\quad (6s,7s)^{2.06}, 6p^{5.45}, 5f^{3.93}, 6d^{1.39}$$

$$NpO_2(NO_3)_3^-\text{:}\quad (6s,7s)^{2.02}, 6p^{5.37}, 5f^{4.16}, 6d^{1.46}$$

---

(13) Desclaux, J. P.; Freeman, A. J. *Handbook on the Physics and Chemistry of the Actinides*; Freeman, A. J., Lander, G. H., Eds.; North-Holland: Amsterdam, 1984; Vol. 1, p 29.

(14) Newman, J. B. *J. Chem. Phys.* **1967**, *47*, 85.

(15) Denning, R. G.; Norris, J. O. W.; Brown, D. *Mol. Phys.* **1982**, *46*, 287.

(16) Alcock, W. N.; Roberts, M. M. *J. Chem. Soc., Dalton Trans.* **1982**, 33.

(17) Barclay, G. A.; Sabine, T. M.; Taylor, J. C. *Acta Crystallogr.* **1965**, *19*, 205.

(18) Hall, D.; Rae, A. D.; Waters, T. N. *Acta Crystallogr.* **1966**, *20*, 160.

(19) Cook, M.; Case, D. A. *QCPE* **1982**, *14*, 465.

(20) Schwarz, K. *Phys. Rev. B: Solid State* **1972**, *5*, 2466.

(21) Norman, J. G., Jr. *J. Chem. Phys.* **1974**, *61*, 4360.

Table IV. Theoretical and Experimental Excitation Energies of $NpO_2Cl_4^{2-}$ (cm^{-1})

orbital	$X\alpha$[a]		$X\alpha + \vec{L}\cdot\vec{S}$	exptl[b]	sym[b]
$1b_{1u}$	0.0	Γ_7	0.0	0.0	Γ_7
$2b_{2u}$	905	Γ_7	1052	~900–1050	Γ_7
$6e_u$	2894	Γ_7	6123	6880	Γ_7
		Γ_6	7984	7890	...
$7e_u$	15129	Γ_6	16122	17241	...
		Γ_7	18844	20080	...
$5a_{2u}$	43708	Γ_6	46344	...	...

$\langle B_4\rangle_{eq} = 2254$, $\langle B_4\rangle_{ax} = 30\,900$, $\langle B_6\rangle_{eq} = 2023$, $\langle B_6\rangle_{ax} = 20\,975$, $\{\langle B_2\rangle_{ax} - \langle B_2\rangle_{eq}\} = 20\,898$, $\zeta(5f) = 1944$

[a] Slater transition-state method. [b] Reference 15.

Table V. Theoretical and Experimental Excitation Energies of $NpO_2(NO_3)_3^-$ (cm^{-1})

orbital	$X\alpha$[a]		$X\alpha + \vec{L}\cdot\vec{S}$	exptl[b]	sym[b]
$9a_1'$	0.0	Γ_7	0.0	0.0	Γ_7
$5e''$	240	Γ_9	64	...	...
		Γ_7	5209	6459	Γ_7
$5a_2'$	6416	Γ_7	9855	9420	Γ_7
$12e'$	17800	Γ_8	18727	17844	Γ_8
		Γ_9	21356	20816	Γ_9
$7a_2''$	54620	Γ_8	57049	...	...

$\langle B_4\rangle_{ax} + {}^9/_{16}\langle B_4\rangle_{eq} = 40\,629$, $\langle B_6\rangle_{eq} = 6355$, $\langle B_6\rangle_{ax} = 28\,690$, $\{\langle B_2\rangle_{ax} - {}^3/_4\langle B_2\rangle_{eq}\} = 26\,178$, $\zeta(5f) = 1907$

[a] Slater transition-state method. [b] Reference 15.

In these complexes Np is expected to exhibit the formal valence configuration $[Rn]d^0f^1$. As suggested before,[4] the increase in orbital population over the formal configuration can be taken as a measure of the individual orbital contribution to bonding. Therefore, we may conclude that the Np 5f orbitals contribute more significantly to the covalent bonding in these systems than do the 6d orbitals. This is apparently a common feature of most of the previous MO calculations of UO_2^{2+} or related compounds.[22-24] However, it is not a general trend in the MO calculations of other actinide complexes.[4]

The f- and d-orbital charges of $NpO_2(NO_3)_3^-$ are greater than those of $NpO_2Cl_4^{2-}$, indicating an increased covalency between Np and the nitrates. Naturally this is anticipated from the Np–O distances used in this work (Np–O in $NpO_2(NO_3)_3^-$ is shorter than Np–O in $NpO_2Cl_4^{2-}$ by 0.018 Å). This is also consistent with the greater Np–O stretching frequency of 960 cm^{-1} in $CsNpO_2(NO_3)_3$ as compared to 919 cm^{-1} in $Cs_2NpO_2Cl_4$.[15]

The neptunyl complexes are supposed to contain an extra electron outside a closed-shell configuration. ESR results[25] have indicated that it has an angular momentum property of an f electron. In agreement with this it can be seen from Tables II and III that the HOMO state is ~100% f in character in both complexes.

There are similarities between our results and other MO calculations of the UO_2^{2+} ion.[22-24,26] For example, the strong interaction reported previously between U 6p and O 2s orbitals in UO_2^{2+} are also exhibited in our calculations mainly in the valence levels $1a_{2u}$, $2a_{2u}$ in $NpO_2Cl_4^{2-}$ and $1a_2''$, $2a_2''$ in $NpO_2(NO_3)_3^-$.

In our systems, the MOs corresponding to the four highest occupied levels of UO_2^{2+} have the energy order

$$NpO_2Cl_4^{2-}:\ 3\sigma_g^+ < 3\sigma_u^+ < 1\pi_g < 2\pi_u$$

$$NpO_2(NO_3)_3^-:\ 3\sigma_g^+ < 3\sigma_u^+ < 2\pi_u < 1\pi_g$$

These levels are mainly derived from the axial oxygen 2p orbitals, in accordance with other MO calculations of the uranyl ion.[23,24,26] The REX method[22] as applied to UO_2^{2+} and $UO_2Cl_4^{2-}$ leads to a somewhat different situation, where the HOMO of these ions ($3\sigma_u^+$) turns out to be one of the f-like MOs. Because these levels are close in energy, there is no agreement among the different MO approaches as to their ordering. RXα calculations of the UO_2^{2+} ion[23] have shown that these orbitals change ordering with decreasing bond distance.

The energies of the Cl 3p-like MOs of $UO_2Cl_4^{2-}$ are located between the $2\sigma_u^+$ and $3\sigma_g^+$ MOs of the UO_2^{2+} moiety as determined by the REX method.[22] In $NpO_2Cl_4^{2-}$ our results show that all the levels derived from the Cl 3p orbitals lie immediately below the HOMO state ($1b_{1u}$).

The MOs derived from the orbitals of the equatorial ions (Cl^-, NO_3^-) are almost of localized nature, i.e., they involve weak interaction with the Np orbitals. This implies that the bondings between NpO_2^{2+} and the Cl^- or NO_3^- ions are essentially ionic.

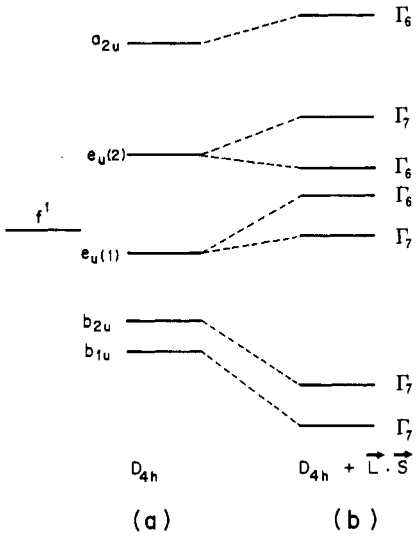

Figure 1. Ground and excited states of $NpO_2Cl_4^{2-}$: (a) without the spin–orbit coupling effect; (b) with the spin–orbit coupling effect.

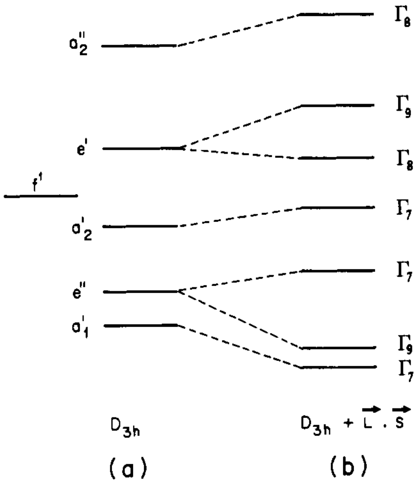

Figure 2. Ground and excited states of $NpO_2(NO_3)_3^-$: (a) without the spin–orbit coupling effect; (b) with the spin–orbit coupling effect.

Ligand Field Spectra. The possible f–f transitions of $NpO_2Cl_4^{2-}$ and $NpO_2(NO_3)_3^-$ complexes (ignoring the spin–orbit coupling effect) were calculated within the Xα method by the Slater transition-state procedure[27] and are given in Tables IV and V (see also Figures 1 and 2).

The potential due to the surrounding ligands affecting the splitting of the metal ion orbitals is usually expanded as a series of spherical harmonics centered on the metal ion:[28]

---

(22) Pyykkö, P.; Lohr, L. L., Jr. *Inorg. Chem.* **1981**, *20*, 1950.
(23) Wood, J. H.; Boring, M.; Woodruff, S. B. *J. Chem. Phys.* **1981**, *74*, 5225.
(24) Walch, P. F.; Ellis, D. E. *J. Chem. Phys.* **1976**, *65*, 2387.
(25) Bowers, K. D.; Owen, J. *Rep. Prog. Phys.* **1955**, *18*, 304.
(26) Tatsumi, K.; Hoffmann, R. *Inorg. Chem.* **1980**, *19*, 2656.
(27) Slater, J. C. *Adv. Quantum Chem.* **1972**, *6*, 1.

$$V(r) = \sum_k \sum_m r^k q_{km} C_m^{(k)}(\theta,\phi) \tag{1}$$

where q_{km} is a function of the ligand coordinates and is given by[28]

$$q_{km} = (4\pi/2k + 1)^{1/2}(Ze^2/a^{k+1})\sum_i Y_k^m(\theta_i,\phi_i) \tag{2}$$

and $C_m^{(k)}$ is the rationalized spherical harmonics[28] having the form

$$C_m^{(k)}(\theta,\phi) = (4\pi/2k + 1)^{1/2}Y_k^m(\theta,\phi) \tag{3}$$

By the aid of group theory the derivation of the potential $V(r)$ in D_{4h} symmetry for f orbitals is straightforward with use of eq 1 and 2:

$$\begin{aligned} V(D_{4h}) = {} & 2\{\langle B_2\rangle_{ax} - \langle B_2\rangle_{eq}\}C_0^{(2)} + \\ & \{2\langle B_4\rangle_{ax} + {}^3\!/_2\langle B_4\rangle_{eq}\}C_0^{(4)} + (70^{1/2}/4)\langle B_4\rangle_{eq}[C_4^{(4)} + C_{-4}^{(4)}] + \\ & \{2\langle B_6\rangle_{ax} - {}^5\!/_4\langle B_6\rangle_{eq}\}C_0^{(6)} - [3(14^{1/2})/8]\langle B_6\rangle_{eq}[C_4^{(6)} + C_{-4}^{(6)}] \end{aligned} \tag{4}$$

Here $\langle B_n\rangle$ stands for the radial integral $Ze^2\langle r^n/R^{n+1}\rangle$; $\langle B_n\rangle_{ax}$ and $\langle B_n\rangle_{eq}$ represent integrals due to the axial and equatorial ligands, respectively.

The potential in D_{4h} involves effectively five radial parameters associated with the operators $C_0^{(2)}$, $C_0^{(4)}$, $C_0^{(6)}$, $C_{\pm4}^{(4)}$, and $C_{\pm4}^{(6)}$. Only four electronic f–f transitions are possible in D_{4h} symmetry. One way to evaluate these parameters is to assume that the ratio $\langle B_4\rangle_{eq}/\langle B_6\rangle_{eq}$ in $NpO_2Cl_4^{2-}$ can be obtained from Xα calculations on the hypothetical octahedral complex $NpCl_6$.[29] In $NpCl_6$ (an f^1 complex) two f–f transitions are possible in O_h symmetry. The Xα transition-state procedure for this molecule gave the values 1643 and 6896 cm^{-1} for the transitions $t_{2u} \leftarrow a_{2u}$ and $t_{1u} \leftarrow a_{2u}$, respectively. These energies correspond to a ratio of $\langle B_4\rangle/\langle B_6\rangle$ equal to 1.114.[30] If this ratio is adopted for the case of $NpO_2Cl_4^{2-}$, one can reduce the number of parameters to four.

Applying the potential of eq 4 to the unperturbed Np^{6+} 5f orbitals, we get the required ligand field matrices in terms of four parameters: $\{\langle B_2\rangle_{ax} - \langle B_2\rangle_{eq}\}$, $\langle B_4\rangle_{ax}$, $\langle B_6\rangle_{eq}$, and $\langle B_6\rangle_{ax}$. If the eigenvalues of the ligand field matrices in D_{4h} are equated to the theoretically calculated values (Table IV), a system of four equations can be formulated involving these parameters. Their values can be obtained from the solution of these equations (Table IV).

Now the 14 f spin orbitals $|m_l^{\pm}\rangle$ of Np^{6+} (where + and − signify $+^1/_2$ and $-^1/_2$ spin) can be simultaneously perturbed by the Hamiltonian $V(D_{4h}) + [\xi(r)]l{\cdot}s$ by using the calculated radial parameters in constructing $V(D_{4h})$. The spin–orbit coupling constant $\zeta(5f)$ was taken as an extrapolated value from known $\zeta(5f)$ values as a function of oxidation states of Np.[13]

The matrices of the D_{4h} double group have been constructed by using the operator $V(D_{4h}) + [\xi(5f)]l{\cdot}s$. The basis functions are the atomic orbitals $|m_l^{\pm}\rangle$ of the Np^{6+} ion. The eigenvalues of these matrices were used to obtain the f–f transition energies in $NpO_2Cl_4^{2-}$ (Table IV). The splitting pattern in D_{4h} as related to that in D_{4h}^* is also shown in Figure 1.

Table VI. Ligand Field Parameters of the f^1 Actinide Chloro Complexes and of $NpO_2Cl_4^{2-}$ As Obtained from RXα Calculations[a]

	M–Cl, Å	metal charge	$\langle B_4\rangle$	$\langle B_6\rangle$
$PaCl_6^{2-}$	2.76	1.65+	2617	1942
UCl_6^-	2.54	2.12+	5074	4205
$NpCl_6$	2.61	2.86+	4080	3661
$NpO_2Cl_4^{2-}$	2.61	2.17+	2254	2023

[a] Parameters for $PaCl_6^{2-}$ and UCl_6^- have been derived from the data of ref 3.

The Xα calculated f–f transitions of $NpO_2(NO_3)_3^-$ are given in Table V.

In D_{3h} the ligand field operator can be formulated as

$$\begin{aligned} V(D_{3h}) = {} & \{2\langle B_2\rangle_{ax} - {}^3\!/_2\langle B_2\rangle_{eq}\}C_0^{(2)} + \\ & \{2\langle B_4\rangle_{ax} + {}^9\!/_8\langle B_4\rangle_{eq}\}C_0^{(4)} + \{2\langle B_6\rangle_{ax} - {}^{15}\!/_{16}\langle B_6\rangle_{eq}\}C_0^{(6)} + \\ & [3(231^{1/2})/32]\langle B_6\rangle_{eq}[C_6^{(6)} + C_{-6}^{(6)}] \end{aligned} \tag{5}$$

Effectively four radial parameters are associated with the operators $C_0^{(2)}$, $C_0^{(4)}$, $C_0^{(6)}$, and $C_{\pm6}^{(6)}$. Because we have also four f–f transitions in D_{3h}, one can proceed directly to calculate these parameters as has been done in the case of $NpO_2Cl_4^{2-}$. In such calculation there is no need to make any assumption regarding these parameters.

The ligand field parameters of $NpO_2(NO_3)_3^-$ calculated by using the same approach adopted in $NpO_2Cl_4^{2-}$ are given in Table V. A simultaneous perturbation ($V(D_{3h}) + [\xi(5f)]l{\cdot}s$) has been also applied for the nitrato complex. The transition energies due to this perturbation are shown in Table V.

As can be seen from Tables IV and V, the spin–orbit coupling perturbation of the relativistic Xα transition energies of $NpO_2Cl_4^{2-}$ and $NpO_2(NO_3)_3^-$ are in better agreement with experimental data than the non-spin–orbit values. A correct ordering of the excited states is also reproduced by using this approach.

The calculated axial parameters are much larger than those for the equatorial ligands. This is a consequence of the strong bonding between Np and oxygen in the NpO_2^{2+} moiety, compared to the weak bonding of Np and the equatorial ligands (Cl^- or NO_3^-). It should be emphasized that $\langle B_6\rangle_{ax}$ in $NpO_2(NO_3)_3^-$ is greater than that of $NpO_2Cl_4^{2-}$ in agreement with our argument concerning the Np–O bond in $NpO_2(NO_3)_3^-$ being stronger than in $NpO_2Cl_4^{2-}$. The relatively large value of $\langle B_6\rangle_{eq}$ of the nitrate ion, ~6360 cm^{-1}, with respect to the value $\langle B_6\rangle_{eq}$ ~2020 cm^{-1} of Cl^- can be explained partly in view of the bidentate action of the nitrate ion in $NpO_2(NO_3)_3^-$ (as has been established from X-ray data[16]) compared to the monodentate action of Cl^-.

Table VI shows a comparison between the radial parameters $\langle B_4\rangle_{eq}$ and $\langle B_6\rangle_{eq}$ obtained in this work for $NpO_2Cl_4^{2-}$ with those obtained[30] from previous Xα calculations[3] on $PaCl_6^{2-}$ and UCl_6^-. As can be seen from this table, the parameters $\langle B_n\rangle$ for the chloride ligand in $NpCl_6$ and NpO_2Cl^{2-} are not in accordance with the general trend[3] $Pa^{4+} < U^{5+} < Np^{6+}$ expected for Np. However, the radial parameters are supposed to be a function of the metal–ligand distance as well as the effective charge on the metal ion. The formation of strong covalent O–Np–O bonding in $NpO_2Cl_4^{2-}$ has the effect of both reducing the effective charge of Np (compare the charge of Np in $NpCl_6$ with that in $NpO_2Cl_4^{2-}$) and elongating the Np–Cl distance relative to the bond distance that would be expected for $NpCl_6$ in a stable configuration.[29] This accounts for the small values reported for $\langle B_4\rangle_{eq}$ and $\langle B_6\rangle_{eq}$ of $NpO_2Cl_4^{2-}$ relative to those of other chloro complexes.

Registry No. $NpO_2Cl_4^{2-}$, 51340-65-9; $NpO_2(NO_3)_3^-$, 54958-87-1.

---

(28) Sugano, S.; Tanabe, Y.; Kamimura, H. *Multiplets of Transition Metal Ions in Crystals*; Academic: New York, 1970; p 7.

(29) SCF relativistic Xα calculations have been performed for $NpCl_6$ by using the same Np–Cl bond length and sphere radii as those used for the $NpO_2Cl_4^{2-}$ ion. The Np–Cl distance used is probably greater than the one that would be estimated for a stable $NpCl_6$.

(30) The radial parameters $\langle B_4\rangle$ and $\langle B_6\rangle$ for $PaCl_6^{2-}$ and UCl_6^- have been derived by using the relations $\langle B_4\rangle = {}^{33}\!/_{154}(3E_2 - E_1)$ and $\langle B_6\rangle = {}^{143}\!/_{154}(E_2 - {}^9\!/_5E_1)$, where E_1 and E_2 are the calculated $t_{2u} \leftarrow a_{2u}$ and $t_{1u} \leftarrow a_{2u}$ transition energies, respectively.